Provided for non-commercial research and education use.
Not for reproduction, distribution or commercial use.

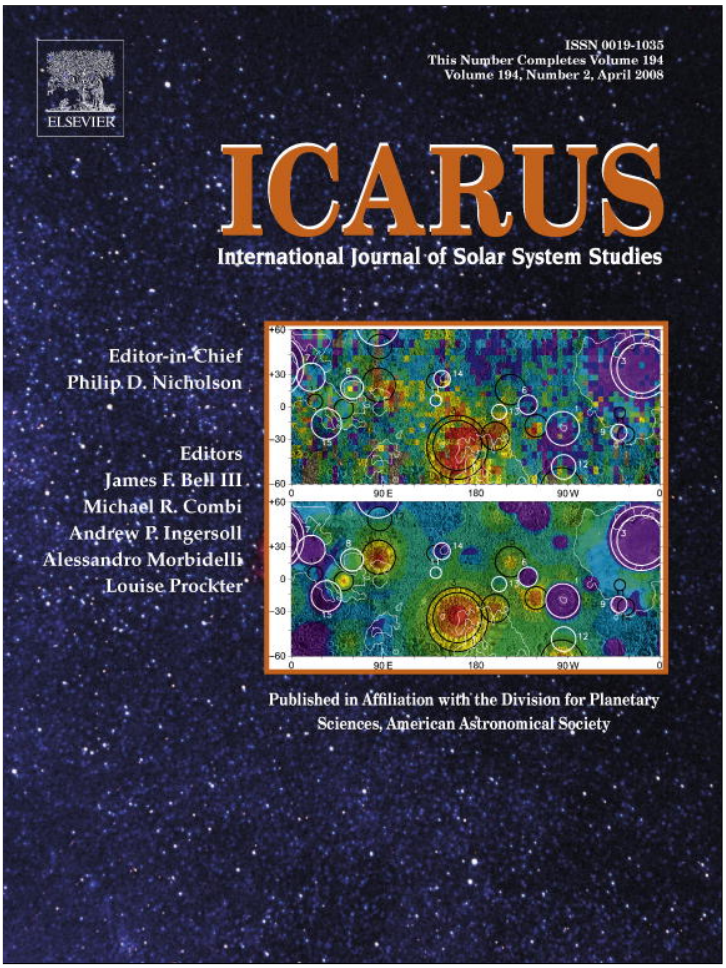

This article appeared in a journal published by Elsevier. The attached copy is furnished to the author for internal non-commercial research and education use, including for instruction at the authors institution and sharing with colleagues.

Other uses, including reproduction and distribution, or selling or licensing copies, or posting to personal, institutional or third party websites are prohibited.

In most cases authors are permitted to post their version of the article (e.g. in Word or Tex form) to their personal website or institutional repository. Authors requiring further information regarding Elsevier's archiving and manuscript policies are encouraged to visit:

http://www.elsevier.com/copyright

Author's personal copy

Available online at www.sciencedirect.com
ScienceDirect
Icarus 194 (2008) 636–646
ICARUS
www.elsevier.com/locate/icarus

Transfer of mass from Io to Europa and beyond due to cometary impacts

José Luis Alvarellos [a,*], Kevin J. Zahnle [b], Anthony R. Dobrovolskis [c], Patrick Hamill [d]

[a] *Space Systems/Loral, 3825 Fabian Way, MS G-76, Palo Alto, CA 94303, USA*
[b] *NASA Ames Research Center, MS 245-3, Moffett Field, CA 94035, USA*
[c] *UCO/Lick Observatory, University of California, Santa Cruz, CA 95064, USA*
[d] *Department of Physics, San José State University, San José, CA 95192, USA*

Received 15 February 2007; revised 24 September 2007

Available online 1 November 2007

Abstract

We simulate the production and orbital evolution of escaping ejecta due to cometary impacts on Io. The model includes the four Galilean satellites, Amalthea, Thebe, Jupiter's gravitational moments, Saturn and the Sun. Five scenarios are examined: an impact at the apex, the sub-jovian point, the anti-jovian point, the antapex, and at the south pole of Io. We estimate that on average a cometary impact injects thrice its mass (in the form of Io surface material) into jovicentric orbit. The majority of the escaping debris comes back to Io, but a sizeable fraction (between 5.0 and 8.7%) manages to reach Europa, and a smaller fraction Ganymede (between 1.5 and 4.6%). Smaller fractions reached Amalthea Thebe, Callisto, and Jupiter itself. For million year time scales, the mass transfer to Europa is estimated as 1.8–3.1 $\times$ 10^{14} g/Myr. The median time for transfer of ejecta from Io to Europa is ~56 years.
© 2007 Elsevier Inc. All rights reserved.

Keywords: Io; Europa; Cratering; Impact processes

1. Introduction

Planetocentric debris are short-lived little moons that are usually fated to be swept up by bigger moons. Obvious sources of planetocentric debris are impact-related. These include satellite disruptions (e.g., Smith et al., 1982), but also less spectacular events in which ejecta from an impact on a moon are launched fast enough to go into orbit about the central planet. The latter scenario should be commonplace in the outer Solar System, where escape velocities are typically much smaller than impact velocities by comets. Planetocentric debris do not generate strong cratering asymmetries (Horedt and Neukum, 1984), and so are relatively more important to trailing hemispheres. Ejecta can be exchanged between moons (e.g., neighboring Galilean satellites; Alvarellos et al., 2002). Impact ejecta from Io are the most plausible source of rocks in Europa's ice shell, and provide an alternative to sputtering as a way to transport sulfur and other elements from Io to Europa.

We report on a set of test particle simulations of impact ejecta generated by comets striking Io. The initial conditions for the ejecta swarm are consistent with impact physics as currently understood. The numerical simulations yield the fraction of material from Io reaching various targets, Europa being the most interesting. In addition, given the cratering rate at Io, the total mass ejected and the fraction of that total mass that escapes Io allow us to calculate the mass transfer rate due to impacts.

In Section 2 we provide details of the initial conditions. In Section 3 we present the results of the numerical simulations. In Section 4 we compute the mass transfer rate from Io to other moons. Finally, in Section 5 we present a discussion and state our conclusions.

2. Impacts and the production of ejecta; initial conditions

We begin by considering impacts of ecliptic comets with the surface of Io. These form the bulk of the impactors responsible for cratering at Jupiter. Ecliptic comets also include the Jupiter Family Comets (Zahnle et al., 1998, 2003). There are no known impact craters on Io, revealing the youthfulness of its surface.

* Corresponding author.
E-mail address: alvarellos.jose@ssd.loral.com (J.L. Alvarellos).

0019-1035/$ – see front matter © 2007 Elsevier Inc. All rights reserved.
doi:10.1016/j.icarus.2007.09.025

Author's personal copy

Table 1
Adopted numerical data for Io. Data come from Jacobson's model (1999), except for Io's crustal density which comes from Zahnle et al. (2003)

Symbol	Meaning	Value
g	Acceleration at the surface	179.7 cm/s^2
$R_{\rm Io}$	Physical radius	1821.3 km
R_H	Hill radius	10,564 km
ρ_t	Crustal density	2.7 g/cm^3
$v_{\rm orb}$	Orbital speed	17.3 km/s
$v_{\rm esc}$	Escape speed	2.558 km/s
$v^*_{\rm esc}$	Effective escape speed; see Eq. (5)	2.345 km/s

Resurfacing rates have been estimated to be as high as 10 cm/yr (Johnson and Soderblom, 1982).

For specificity we define our 'canonical' ecliptic comet as having a diameter d of 1.5 km and density ρ_i of 0.6 g/cm^3 (i.e., $m_i = 1.06 \times 10^{15}$ g). The impact speed of an ecliptic comet with a synchronous satellite is a function of the apex angle β (Zahnle et al., 2001), and is approximated by

$$U \approx \sqrt{3} v_{\rm orb} (1 + 0.9 \cos\beta)^{0.35} \tag{1}$$

(Alvarellos et al., 2005), where $v_{\rm orb}$ is the satellite's orbital speed. After the impact, the resulting transient crater has a diameter given by

$$D_t = 1.1 \left(\frac{U^2}{g}\right)^{0.217} \left(\frac{\rho_i \cos\theta}{\rho_t}\right)^{0.333} d^{0.783} \tag{2}$$

(Housen et al., 1983; Zahnle et al., 2003). Here, g is the acceleration of gravity, ρ_t is the density of the target surface and θ is the incident angle (assumed to be 45° throughout this paper); see parameters listed in Table 1.

We consider five impact geometries: at the apex of motion ($U = 37.5$ km/s, $D_t = 15.5$ km); at the subjovian point, at the antijovian point, and at the south pole of Io (for the latter three cases $U = 30.0$ km/s, and $D_t = 14.1$ km); and at the antapex of Io ($U = 13.4$ km/s, $D_t = 9.9$ km). All else being equal, an impact at the apex produces a larger crater.

Most of the impact ejecta are retained by Io and become the crater's ejecta blanket. In this study we are interested in the ejecta that escape Io to achieve jovicentric orbits. In a previous paper addressing the fate of ejecta escaping from the icy satellites of Saturn (Alvarellos et al., 2005), we considered two models for determining initial conditions of ejecta: the stress-wave spallation model of Melosh (1984, 1985, 1989) and the scaling model of Housen et al. (1983); we follow the same approach in this study. The two different descriptions do not produce markedly different results.

2.1. Scaling/rubble model

In the scaling/rubble model of Housen et al. (1983), the ejecta speed v_e decays as a power law

$$v_e = K \sqrt{g R_t} \left(\frac{x}{R_t}\right)^{-e_x}, \tag{3}$$

where the dimensionless factor K is

$$K = 0.62 \left(\frac{\rho_i}{\rho_t}\right)^{0.2} \approx 0.45\ldots \tag{4}$$

and $e_x = 1.77$ (Alvarellos et al., 2005), $R_t = D_t/2$, and x is the distance from the center of the crater.

Housen et al. (1983) predict constant ejection angles, while Cintala et al. (1999) provide experimental evidence (by studying impacts into sand targets) for Housen et al.'s scaling model. In a study of the fate of ejecta from Ganymede (Alvarellos et al., 2002), we found that our results were insensitive to the ejection angles. In this study, we assume the ejection angle is 45° for simplicity. This model of ejection is applicable to "incompetent" surfaces, such as those composed of regolith. We refer to this as the "rubble" model; it is of questionable relevance to Io, whose surface seems mostly made of hard rock. In addition, laboratory calibration of this model is available for the range $0.2 < x/R_t < 0.9$, while in this paper the rubble ejecta are lofted from a region of $x/R_t \approx 0.11$ (i.e., close to the impactor in order to achieve speeds high enough to escape). Nevertheless, we decided to keep the rubble results as representative of the low speed limit of ejecta cases, but due to the 'basaltic' nature of the surface of Io the spall model may be the more appropriate case.

2.2. Spall model

The "spall" model is more applicable to competent or "hard" targets. In the stress-wave model of spallation (Melosh, 1984), an impact is considered analogous to an underground explosion (at a depth roughly equivalent to a cometary diameter) that generates a radially propagating compressive wave. Upon its reaching the ground, a shear and a tensile wave are reflected back into the surface. Interference between the three waves results in an uncompensated outward motion of the surface. At the surface itself pressures cancel; however the pressure gradient is enormous, resulting in the ejection of slab-like, competent pieces of the target called spalls. The ejection velocity in the spall model results from the vector addition of the three wave velocities. It is a function of several variables including comet's size, density, and impact speed; it is also a function of target properties such as its density and Poisson ratio. In addition, this model also predicts that the ejection angles vary as a function of distance from the center of the crater. In general, the closer to the impact point, the more nearly vertical is the ejection. We assume the surface of Io consists of rock and apply the spall model accordingly. Throughout this paper, whenever we use the term "spallation/spall model" we refer to the stress-wave version of the spallation model; see Melosh (1984, 1985, 1989) for details. The Appendix of Alvarellos et al. (2005) contains a simplified explanation, but note that we have implemented the Zahnle et al. (2008) modification for the particle speed [i.e., we use $2/(\sqrt{\rho_t/\rho_i} + 1)$ as coefficient for the particle velocity v_p, rather than (ρ_i/ρ_t) in Eq. (A.4) of Alvarellos et al. (2005); see Zahnle et al. (2008), Eq. (14)].

2.3. Initial conditions in a topocentric system

We address only those ejecta whose speeds allow them to escape Io. In the two-body problem, a particle escapes to infinity if its ejection speed v_e exceeds the classical escape velocity

Author's personal copy

Table 2
Satellite masses, radii and orbital elements; the values of GM_m and R_m are from Jacobson et al. (1999). Orbital elements are from Murray and Dermott (1999). The semi-major axes are given in kilometers as well as in Jupiter radii (in parentheses). For Jupiter we use $GM_J = 1.2668653 \times 10^8$ km^3/s^2; $R_J = 71{,}398$ km. Jupiter's oblateness terms are $J_2 = 0.014736$, $J_4 = -0.000587$, $J_6 = 3.1 \times 10^{-6}$, $J_8 = -2.41 \times 10^{-6}$, $J_{10} = 0.24 \times 10^{-6}$, $J_{12} = -0.03 \times 10^{-6}$

Satellite	GM_m (km^3/s^2)	R_m (km)	a_m (km, R_J)	e_m	i_m (°)	P_m (days)
Amalthea	0.138	83.5	181,300 (2.54)	0.003	0.4	0.498179
Thebe	0.05	49.3	221,900 (3.11)	0.015	0.8	0.6745
Io	5959.7	1821.3	421,600 (5.90)	0.0041	0.040	1.769138
Europa	3202.7	1565.0	670,900 (9.40)	0.0101	0.470	3.551810
Ganymede	9887.8	2634.0	1,070,000 (14.99)	0.0015	0.195	7.154553
Callisto	7179.3	2403	1,883,000 (26.37)	0.0070	0.281	16.689018

$v_{\rm esc} = \sqrt{2GM_m/R_m}$, where M_m and R_m are respectively the mass and radius of the source body. But because of three-body effects, a particle ejected from a moon may be considered to escape if it reaches the satellite's Hill sphere. The escape criterion becomes $v_e > v^*_{\rm esc} = \gamma v_{\rm esc}$, where the dimensionless correction factor

$$\gamma \approx \sqrt{\frac{2-2\chi}{2-\chi^2}} < 1 \tag{5}$$

depends on $\chi \equiv R_m/R_H$, the ratio of the satellite's physical radius R_m to its Hill radius R_H (Alvarellos et al., 2002, 2005). If χ is small, γ tends to unity and the classical result is recovered, but if χ is large (i.e., approaches one), γ is small. For Io, $\chi \approx 0.1724\ldots$, so $\gamma \approx 0.9166$, while $v_{\rm esc} \approx 2.558$ km/s, so the effective escape velocity $v^*_{\rm esc}$ is only ~2.345 km/s.

Given the impactor's size, its speed and the resulting crater size, we construct ejecta initial conditions in a topocentric frame[1] in the form of test particles arranged in concentric circles inside the crater (see Alvarellos et al., 2005). For each of the cometary impact geometries, the topocentric initial conditions for 600 ejecta particles are translated and rotated to the jovicentric coordinate system and fed into a suitable integrator (along with the jovian model, described in the next section).

We did not consider ejection of 'rubble' from the antapex of Io because in this case our ejection models predict that maximum ejection speeds $v_e > v^*_{\rm esc}$ are reached only inside the footprint of the impactor (i.e., only for $x < d/2$). Such near-field ejecta (jetted target and parts of the impactor itself) are likely to be of some importance but lie beyond the scope of this paper. However, spalls are ejected fast enough to escape from the antapex.

2.4. The jovian model

We use the Swift integrator of Levison and Duncan (1994) to simulate the orbits of the ejecta swarms escaping from Io. Swift is a regularized, mixed-variable symplectic (RMVS) integrator that implements the Wisdom and Holman's (1991) algorithm; for our studies we use the RMVS3 version. It is especially well suited for the interactions of massless test particles with massive bodies.

[1] The origin is the center of the crater, and the x_1, x_2 and x_3 axes point to the local south, east and zenith, respectively.

We have modified Swift to take into account several of Jupiter's higher order oblateness terms (Dobrovolskis and Lissauer, 2004): J_2, J_3, J_4 and J_6 are from Campbell and Synnot (1985); J_8 and J_{10} are from Gavrilov and Zharkov (1977), while J_{12} is extrapolated from the latter source. The Galilean satellite initial conditions are from the JUP147 model (Jacobson et al., 1999). Our model also includes the two largest inner jovian satellites Thebe and Amalthea; their initial conditions are from the JUP230 model (R.A. Jacobson, personal communication). Both sets of initial state vectors are expressed in barycentric, J2000 coordinates for the Epoch 16.0 January 1997. Our model also includes the gravitational effects of the Sun plus the terrestrial planets, modeled as a point mass at the barycenter of the inner Solar System (initial conditions from the JPL DE200 ephemeris). All of the initial conditions are then rotated to Jupiter's equatorial frame of date; the orientation of the pole of Jupiter is from Jacobson et al. (1999), which once computed is assumed constant for the duration of the integrations. Masses and radii are also from Jacobson et al. (1999). Table 2 provides an overview of the Jupiter system used in this study. We did not take into account the effects of solar radiation pressure or Lorentz forces, which are important for micrometer-sized dust particles; here we are concerned with the fate of cm-sized and larger ejecta. Krivov et al. (2002) studied the dynamics of dusty ejecta from the Galilean satellites and found their results consistent with Galileo dust measurements; however, in their study they did not provide ejecta lifetimes or fates.

We tested our configuration of the jovian system by checking the behavior of the Laplace resonant argument

$$\Phi = \lambda_1 - 3\lambda_2 + 2\lambda_3, \tag{6}$$

where the λ_j represent the mean longitudes of Io, Europa and Ganymede, respectively. These three satellites are locked in a 1:2:4 triple mean-motion resonance. We confirmed that the resonant argument in our jovian model librates around 180° with small amplitude and appropriate period (Lieske, 1998; Murray and Dermott, 1999).

3. Integrations and the fate of ejecta

Once the initial conditions of the ejecta particles are computed (rubble or spallation model), they are fed into Swift along with those of the massive bodies and integrated for 10,000 years. As in our previous studies, we ignore particles that come back to Io in less than 3.54 days (i.e., twice Io's orbital period).

Author's personal copy

Table 3
Fates of ejecta escaping from Io for various cases, after 10,000-year integrations. Percentages are normalized to the number of ejecta particles which reach jovicentric orbit (last column). Percentages may not add up to 100 due to round off

Source	Ejecta type	Hit Jupiter	Hit Amalthea	Hit Thebe	Hit Io	Hit Europa	Hit Ganymede	Hit Callisto	Heliocentric space	Still active	Jovicentric (P_0)
Apex	Rubble	0	0	0	518 (92.2%)	37 (6.6%)	7 (1.2%)	0	0	0	562 (100%)
	Spalls	2 (0.3%)	0	0	451 (78.7%)	70 (12.2%)	46 (8.0%)	4 (0.7%)	0	0	573 (100%)
Sub-jovian point	Rubble	0	0	1 (0.2%)	420 (92.3%)	24 (5.3%)	8 (1.8%)	1 (0.2%)	0	1 (0.2%)	455 (100%)
	Spalls	0	2 (0.3%)	1 (0.2%)	498 (86.2%)	46 (8.0%)	28 (4.8%)	2 (0.3%)	1 (0.2%)	0	578 (100%)
Anti-jovian point	Rubble	0	0	0	414 (93.7%)	22 (5.0%)	6 (1.4%)	0	0	0	442 (100%)
	Spalls	2 (0.3%)	1 (0.2%)	1 (0.2%)	483 (83.3%)	62 (10.7%)	29 (5.0%)	2 (0.3%)	0	0	580 (100%)
South pole	Rubble	0	0	0	508 (95.0%)	17 (3.2%)	8 (1.5%)	2 (0.4%)	0	0	535 (100%)
	Spalls	3 (0.5%)	0	0	505 (86.0%)	46 (7.8%)	27 (4.6%)	4 (0.7%)	1 (0.2%)	1 (0.2%)	587 (100%)
Antapex	Rubble[a]	n/a	n/a	n/a	n/a	n/a	n/a	n/a	n/a	n/a	n/a
	Spalls	0	0	0	538 (94.2%)	28 (4.9%)	4 (0.7%)	0	1 (0.2%)	0	571 (100%)
Combined	Rubble	0	0	1 (0.05%)	1860 (93.3%)	100 (5.0%)	29 (1.5%)	3 (0.15%)	0	1 (0.05%)	1994 (100%)
	Spalls	7 (0.24%)	3 (0.10%)	2 (0.07%)	2475 (85.7%)	252 (8.7%)	134 (4.6%)	12 (0.42%)	3 (0.10%)	1 (0.03%)	2889 (100%)

[a] Rubble ejecta cannot escape from the antapex.

These are either particles that go into suborbital trajectories or particles trapped in temporary chaotic orbits about Io (Alvarellos et al., 2002, 2005).

As a specific example, let us consider the results of an integration of ejecta resulting from a cometary impact at the apex of Io. For the particular case of ejection using the spall model, ejection speeds at the surface ranged from 2.38 to 8.54 km/s ($1.0v^*_{esc}$ to $3.6v^*_{esc}$); 27 test particles came back to Io in less than 3.54 days, leaving 573 particles in jovicentric orbits. After 10,000 years were there no particles still in orbit about Jupiter. Two particles struck Jupiter but none hit the small inner moons Amalthea and Thebe. No particles escaped the Jupiter system, escape being defined as wandering beyond Jupiter's Hill radius (∼0.36 AU). The majority (451, or 78.7%) came back to Io. Of the rest, 70 (12.2%) reached Europa, 46 (8.0%) reached Ganymede and just four (0.7%) hit Callisto. These results are summarized in Table 3, along with results for jovicentric orbit injection from Io for the other hypothetical crater sources, using both the rubble and spallation models.

In general most of the jovicentric Io ejecta returns to Io. This is consistent with previous, similar studies where the source moon re-accretes most of its own debris (Soter, 1971; Burns and Gladman, 1998; Alvarellos et al., 2002, 2005). This is not surprising because these particles start on Io-crossing orbits, which have a high probability of removal by the source moon (Hamilton and Burns, 1994; Burns and Gladman, 1998). In fact, we expect that recaptured ejecta from the apex (antapex) of Io will tend to accumulate on its trailing (leading) side (Alvarellos et al., 2002, 2005).

In the rubble model we find that, on average, 5.0 and 1.5% of escaping Ionian material reaches Europa and Ganymede, respectively. In comparison, in the spall model, the fractions reaching Europa and Ganymede increase to 8.7 and 4.6%, respectively, with even distant Callisto receiving 0.42%. A wider dispersion is expected, since in general, the spallation model produces faster ejection speeds than the rubble model.

A relevant comparison is to the work of Zeehandelaar and Hamilton (2007) where the authors, motivated by Pioneer 10 and 11 dust detections, computationally simulated the evolution of collisional dust grains launched radially outward from all four Galilean satellites at the satellites' escape speeds. In addition to gravitational forces, Zeehandelaar and Hamilton (2007) also took into account solar radiation pressure and Lorentz forces, as these are important for modeling dust-sized particles. They modeled the Galilean satellite orbits as circular, uninclined orbits. Only the J_2 term of Jupiter's oblateness was taken into account. In spite of these differences, their results are similar to ours: they found that 4.8% of material from Io reached Europa, while 1.2% reached Ganymede and none reached Callisto.

In Fig. 1 we plot the distribution of transfer times for ejecta reaching Europa. The quickest journey from Io to Europa was 179 days, made by a rubble particle from the apex of Io. The median time to get from Io to Europa was 56 years, while the mean time was 146 years. As discussed in Dobrovolskis et al. (2007), the distribution shown in Fig. 1 is the absolute derivative of the decay curve for these (Europa-bound) ejecta. A similar analysis of the distribution of transfer times from Io to Ganymede yields the median (168 years) and the mean (534 years) transfer times. In Fig. 2 we plot the orbital evolution of an exemplary ejectum that reached Europa after 63.6 years. This particle spent most of its time in an Europa-crossing orbit.

The locations of the impact sites on Europa are shown in Fig. 3. These are not wholly random, but instead show a preference for the leading side of Europa. This is to be expected, since particles on a transfer orbit from Io to Europa should be traveling slower than Europa when it encounters them so that the debris should, on average, accumulate on the leading side. The distribution of impact speeds is shown in Fig. 4. The mean and median impact speeds for pieces of Io raining down on the surface of Europa are 4.2 and 3.7 km/s, respectively; however,

Author's personal copy

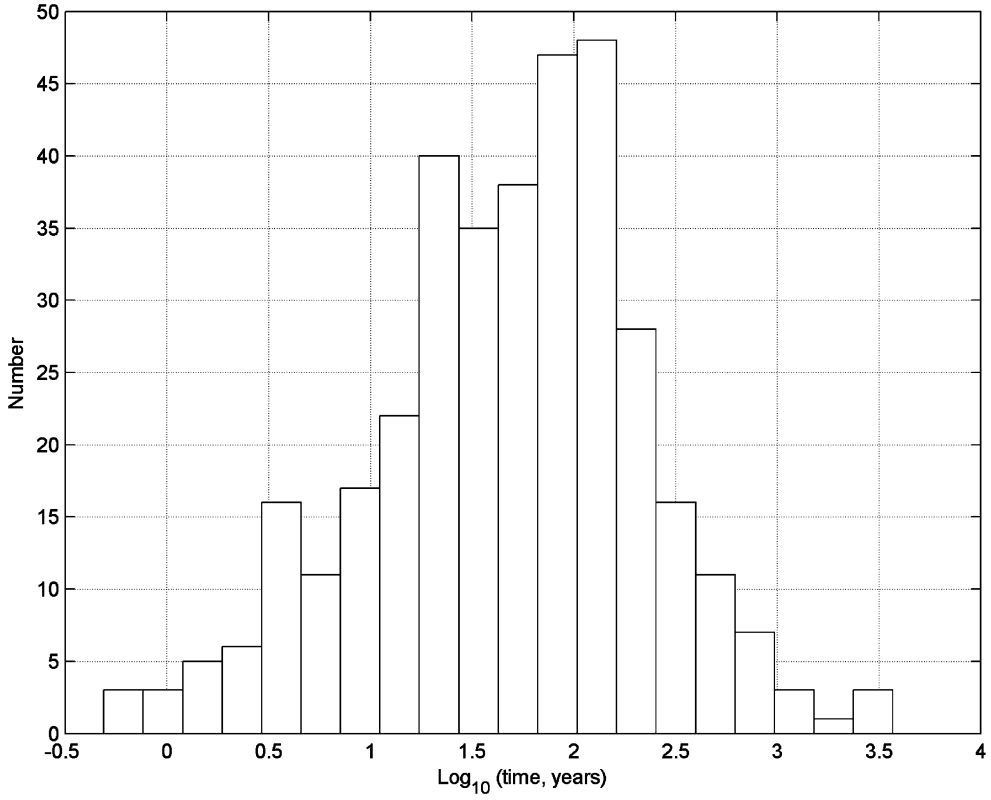

Fig. 1. Distribution of transfer times of ejecta from Io to Europa (all cases combined); see text for details.

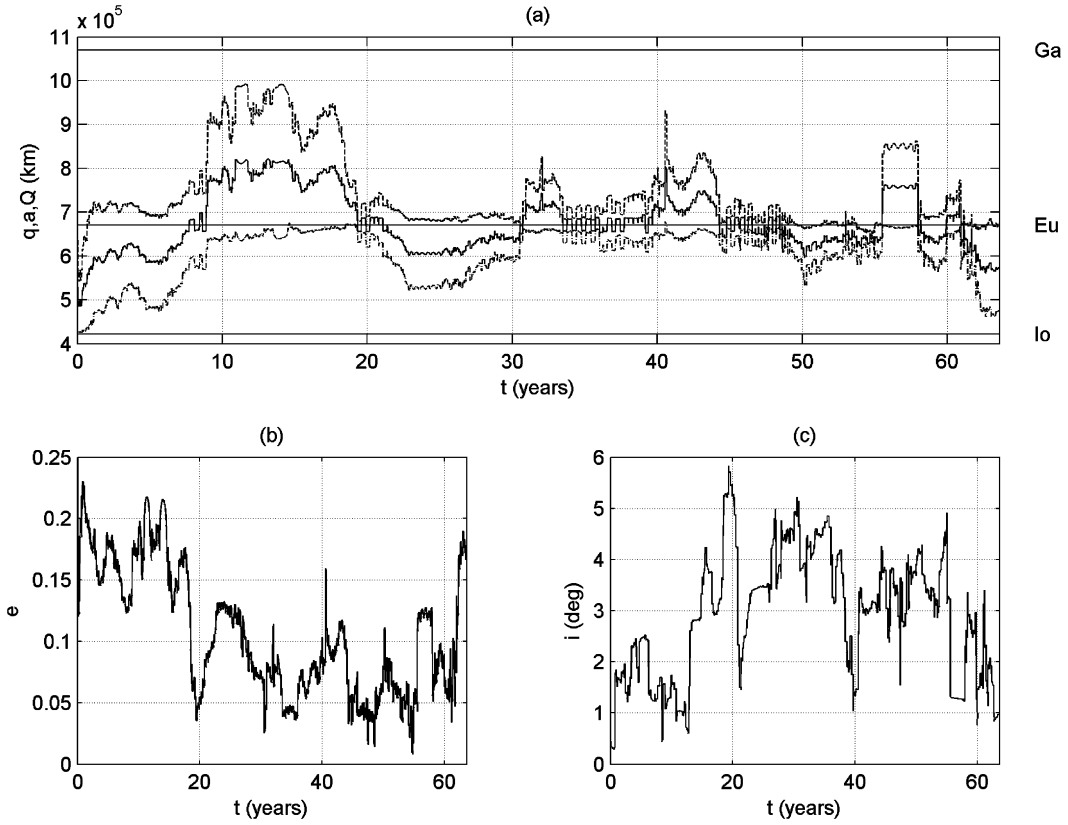

Fig. 2. Evolution of the orbital elements of an ejectum from the antijovian point of Io that reached Europa. This particle spent most of its free time in a Europa-crossing orbit. (a) Semi-major axis, periapse, and apoapse vs time. Note that the particle is briefly trapped in a 5:6 resonance with Europa for $55 < t < 58$. (b) Eccentricity vs time. (c) Inclination vs time.

Author's personal copy

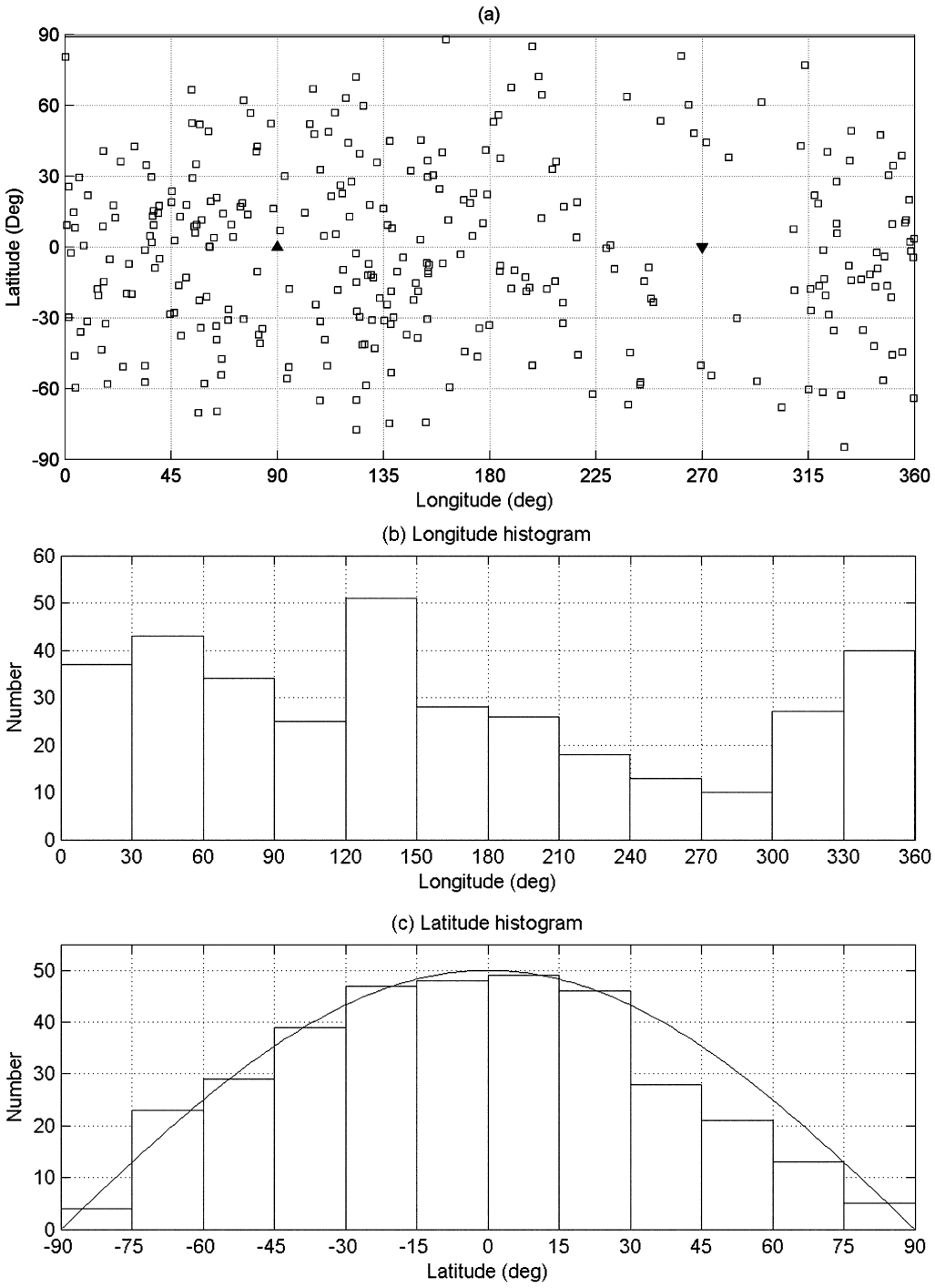

Fig. 3. (a) Impact sites of Ionian ejecta on Europa. The sub-Jupiter point is located at the origin. The leading hemisphere runs from 0 to 180°, while the trailing hemisphere runs from 180 to 360°. The upward-pointing triangle represents the apex of motion, while the downward pointing triangle represents the antapex. (b) Histogram of impact longitudes; there is a clear preference for the leading side of Europa, as expected. (c) Histogram of impact latitudes; because there is less surface area in each latitude band as one moves away from the equator, the poles are less likely to get hit. The curve is the function $f = 50\cos(\phi)$, where ϕ is latitude.

there were a handful of fast impactors at the tail end of the distribution reaching impact speeds above 10 km/s.

We found a few cases where material was transferred to Jupiter's small, reddish inner moons Thebe and Amalthea. Indeed, all of the test particles reaching this pair of moons were spalls, which is not surprising given that the spall model produces faster ejection speeds.

After 10,000 years the number of escaped ejecta still orbiting Jupiter has been drastically reduced. Fig. 5 shows the depletion of the ejecta population as a function of time. Notice the rapid decline: the fraction of the original material remaining is reduced to less than 50% in a time frame ranging from 1 to 15 years; it can be seen also that the rubble ejecta disappear somewhat faster than the spalls. Dobrovolskis et al.

Author's personal copy

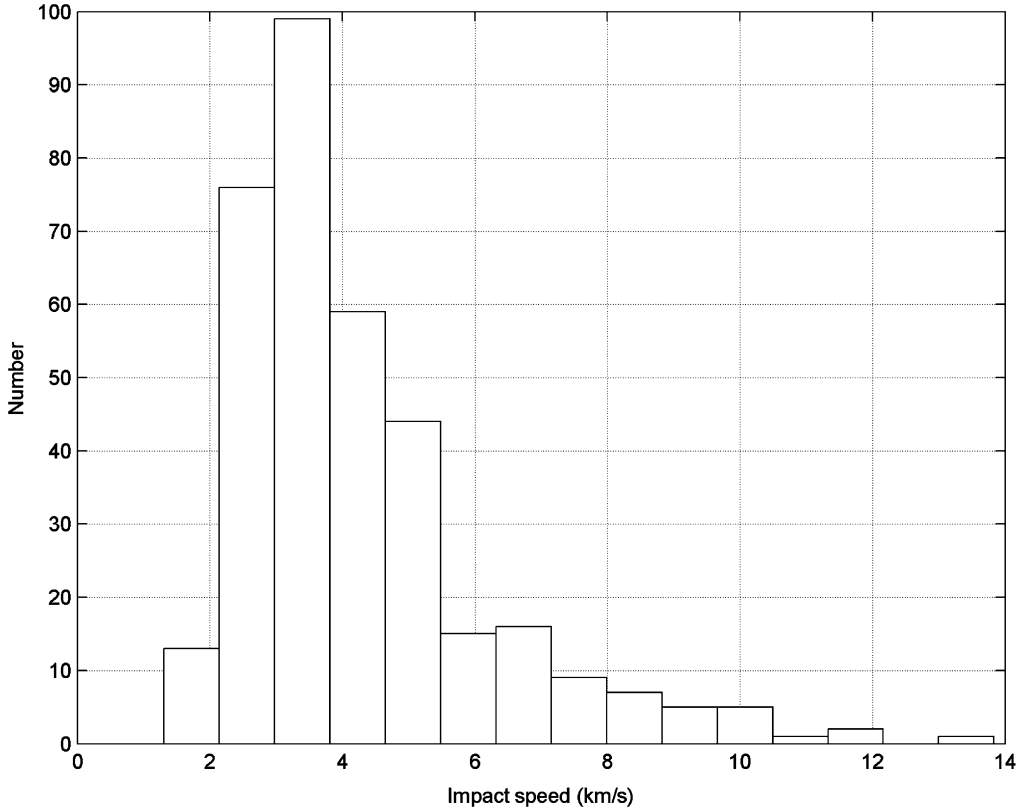

Fig. 4. Distribution of impact speeds on Europa for ejecta from Io (all cases combined).

(2007) have analyzed in detail several particle population decay curves, including some of the cases presented here. The decay is not simply exponential, but it is better described by a 'stretched/exponential' law, for which the longer-lasting particles have generally longer half-lives. The functional form of the decay curves is well approximated by

$$P(t) = P_0 \exp\left(-\left[\frac{t}{t_0}\right]^{\beta}\right), \tag{7}$$

where $P(t)$ is the particle population at time t, P_0 is the original population (see Table 3), t_0 is the time needed for the original population to decay to $e^{-1}P_0 \approx 0.368P_0$ and β is a dimensionless exponent (Dobrovolskis et al., 2007). The parameters for our Io-ejecta decay curves span the ranges $3 < t_0 < 46$ years and $0.32 < \beta < 0.51$, with the spalls typically having the higher values in both t_0 and β; note that the latter implies that the decay of the rubble ejecta deviates more from simple exponential decay than that of the spalls (i.e., the closer β is to unity, the closer the decay resembles simple exponential decay).

Of the 4883 total ejecta particles that went into jovicentric orbit, only two survived the 10,000 year integrations. One survivor was a rubble particle ejected from the subjovian point of Io, while the other was a spall particle ejected from the south pole. The original orbits of these two particles (indeed, all Io ejecta) originally had perijoves very similar to the semi-major axis of Io; repeated encounters with the Galilean moons eventually raised their semi-major axes, eccentricities and inclinations. Ejecta gradually got culled by (mostly) Io and the other moons, until eventually only these two were left. Their relatively high inclinations improve their chances for survival; however, the long term prospects do not look good, since at the end of the integrations both were left in Callisto and/or Ganymede-crossing orbits; see Fig. 6.

4. Mass transfers

In this section we address how much mass can be transferred (by impacts) from Io to Europa and other moons. To do so we must answer the following questions: How much total mass is excavated by the impact process? What fraction of this mass escapes Io? Finally, to compute a mass transfer rate we must address the issue of cratering rates at Io.

4.1. Total mass excavated

Based on the work of Schmidt and Housen (1987), and of Melosh (1989), Zahnle et al. (2003) modified the concept of 'apparent volume' $V_{\rm ap}$ with the incident impact angle as (all cgs units)

$$V_{\rm ap} = 0.13\left(\frac{m_i}{\rho_t}\right)^{0.783}\left(\frac{\rho_i}{\rho_t}\right)^{0.217}\left(\frac{U^2}{g}\right)^{0.65}\cos\theta. \tag{8}$$

Apparent volume is measured with respect to the original surface. Therefore we use for the total ejected mass

$$m_{\rm ej} = \rho_t V_{\rm ap}. \tag{9}$$

Thus, for example, we see that an impact at the apex of motion ejects a total of $m_{\rm ej} \sim 5.8 \times 10^{17}$ g, impacts at the subjovian,

Author's personal copy

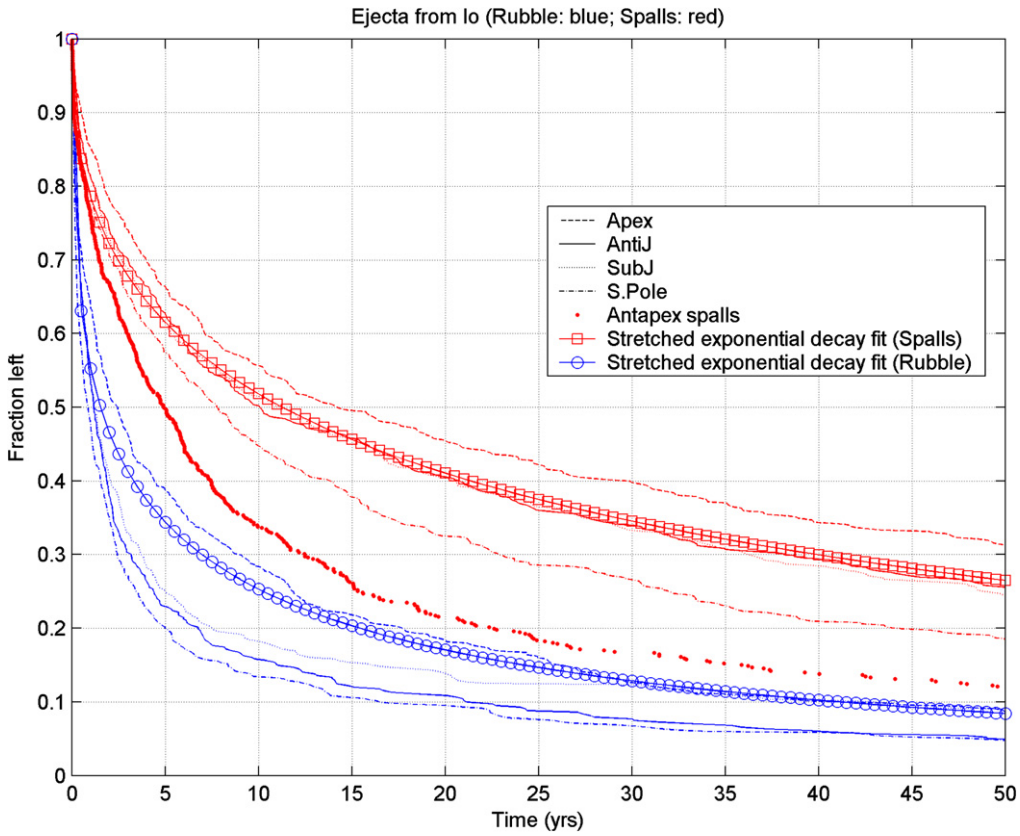

Fig. 5. Decay of the population of jovicentric Io ejecta as a function of time (blue is for rubble, red is for spalls). The curves follow a stretched-exponential decay law; $t_0 = 4.19$ years and $\beta = 0.37$ are the parameters for the combined rubble run fit, while $t_0 = 26.1$ years and $\beta = 0.44$ are the parameters for the combined spall run fit. Half-lives range from 1 year to 15 years; this implies that the south pole rubble (quickest decay) and the apex spalls (slowest decay) form an envelope that describes the decay behavior of all Io ejecta.

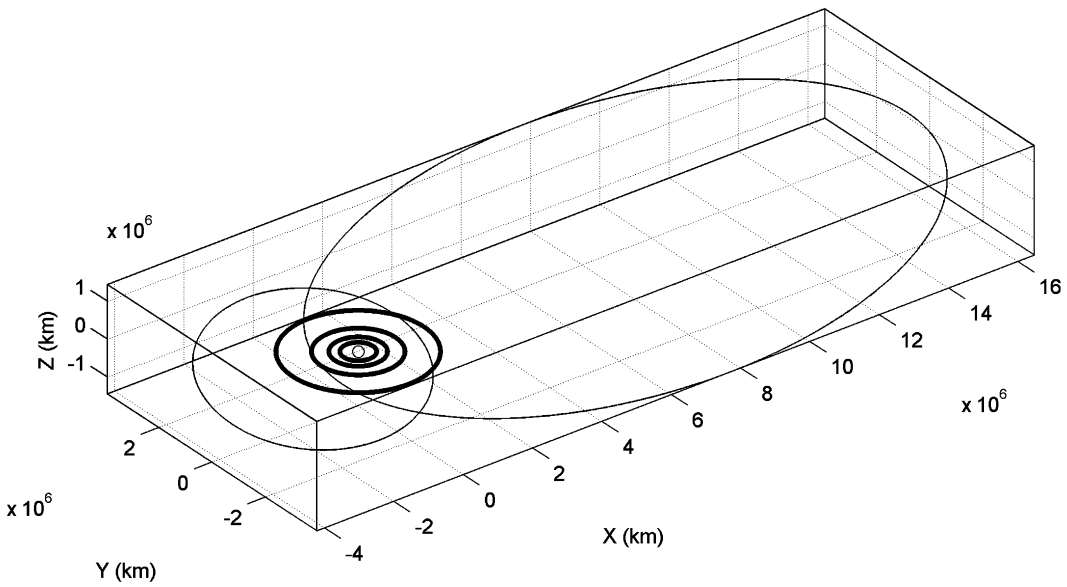

Fig. 6. The osculating prograde orbits of the only two survivors at $t = 10{,}000$ years. The four inner circles show the orbits of Io, Europa, Ganymede and Callisto, respectively. The smaller of the two orbits corresponds to the sole rubble survivor ($q = 1.60 \times 10^6$ km, $Q = 4.21 \times 10^6$ km and $i = 16.7$ degrees); note that it is on a Callisto-crossing orbit. The second, larger orbit corresponds to the sole spall survivor ($q = 1.07 \times 10^6$ km, $Q = 16.5 \times 10^6$ km and $i = 20.1$ degrees). This latter particle's orbit crosses the orbits of both Ganymede and Callisto; indeed note that it is strongly interacting with Ganymede. The eccentricity vectors of these two orbits were artificially placed 180 degrees apart for clarity. The odds of long-term survival for both particles are slim.

Author's personal copy

antijovian and s. pole eject $m_{ej} \sim 4.1 \times 10^{17}$ g, and an impact at the antijovian point ejects only $m_{ej} \sim 1.5 \times 10^{17}$ g ($\theta = 45°$). Note that these values are more than two orders of magnitude greater than that of our canonical comet.

4.2. Escaping ejecta mass

Based on the work of Housen et al. (1983), Veverka et al. (1986) suggest that the fraction of ejecta with speed faster than v can be written

$$F(v) = C_2 \left(\frac{v}{\sqrt{g D_t}} \right)^{-b}, \tag{10}$$

where C_2 and b are dimensionless constants; for rock Veverka et al. (1986) give $C_2 = 0.6$ and $b = 1.7$. For self-consistency with our Eqs. (2) and (8) we use $b = 1.66$. Equations (2), (8)–(10) together imply that

$$m_{esc} = 0.1 C_2 m_i \left(\frac{\rho_i}{\rho_t} \right)^{0.277} \left(\frac{U}{v_{esc}^*} \right)^{1.66}. \tag{11}$$

The mass of ejecta that escapes is directly proportional to the projectile mass if the impact velocity and the projectile and target densities are held fixed. For our specific case of impacts into Io, $m_{esc} = 5 C_2 m_i = 3 m_i$ (see Zahnle et al., 2008).

4.3. Zunil analog

Another source of information is the martian impact crater Zunil (McEwen et al., 2005). Zunil is a very young 10.1 km crater set in young martian lavas, and its secondary craters are distinctive and numerous. Zunil is an excellent analog to impact craters on Io, both in its size and in the nature of the target material. Through its secondaries it is an excellent source of ground truth bounding the spall production process. Elsewhere (Zahnle et al., 2008) we argue from McEwen et al.'s (2005) numerical models that the Zunil impact event ejected 3.8× the mass of the 4×10^{14} g comet that created the crater.

Although obtained using an entirely different argument, the ratio of escaping mass to comet mass is quite similar to what we obtained by extrapolating the excavation flow to Io's escape velocity (Eq. (11)). It is not clear to us whether this agreement stems from some deeper connection between the spalls and the excavation flow, or whether it is just coincidence. In any event, for our purposes we will accept the estimate that a comet striking Io typically ejects thrice its mass into orbit about Jupiter in the form of basaltic rocks.

4.4. Mass transfer per impact

Our numerical experiments simulate the orbital evolution of the small subset of ejecta that escape Io. Knowing the total ejecta mass that escapes and that reaches certain targets, it is then easy to compute the total mass transferred per impact. For transfer of mass from Io to Europa we obtain

$$\Delta m_{12} = f_{12} m_{esc} \approx [1.6\text{–}2.8] \times 10^{14} \text{ g} \tag{12}$$

Table 4
Mass transfer rates due to impacts on Io; all rates are in grams per Myr

Target	$\dot{m}$ (rubble)	$\dot{m}$ (spalls)
Europa	1.8×10^{14}	3.1×10^{14}
Ganymede	0.5×10^{14}	1.6×10^{14}
Callisto	0.5×10^{13}	1.5×10^{13}
Jupiter[a]	$<1.8 \times 10^{12}$	8.6×10^{12}
Amalthea[a]	$<1.8 \times 10^{12}$	3.7×10^{12}
Thebe	1.8×10^{12}	2.4×10^{12}

[a] For these null rubble results the transfer efficiency has been computed as being $f < 1994^{-1} \sim 0.0005$.

per impact, depending on whether we assume the rubble or spall model ($f_{12} = 0.050$ or 0.087, respectively; see Table 3). For mass transfers to Ganymede we proceed similarly and obtain

$$\Delta m_{13} = f_{13} m_{esc} \approx [0.5\text{–}1.5] \times 10^{14} \text{ g} \tag{13}$$

per impact, again depending on the ejection model adopted ($f_{13} = 0.015$ or 0.046, respectively). We can use the same method when computing mass transfers to the other moons.

4.5. Absolute transfer rate

To convert these numbers to a mass transfer rate we need to know the cratering rate at Io. For crater sizes relevant to this study ($D_t > 10$ km), Zahnle et al. (2003) estimate that the cratering rate of ecliptic comets at Io is 2.7×10^{-14} per km^2 per year, uncertain to a factor of three. Multiplying this quantity by the surface area of Io and taking the reciprocal, we find that Io gets hit by a 1.5-km-size ecliptic comet once every ∼900,00 years. This, then, is the time-scale needed to convert our mass transfer rates to an absolute scale. Results are summarized in Table 4. Recall that most of this mass is transferred relatively soon after the impact: for example, 50% of the ejecta from Io that reaches Europa does so in ∼56 years.

It is instructive to compare these transfer rates to other mass flux values. For example, the meteoroid flux at Europa is 45 g/s, or 1.4×10^{15} g/Myr (Johnson et al., 2004); this is more than the Io-ejecta "flux" at Europa. However, on longer time-scales, the latter become relatively and absolutely more important because the largest impact that can occur is progressively larger. In Zahnle et al. (2008) we address this issue in detail.

5. Discussion and conclusions

In this paper we examine the fate of escaping material ejected from the surface of Io due to the impact of a 1.5 km comet. In fact, we estimate that on Io, a comet impact will inject $\sim 3 m_i$ of target material into jovicentric orbit. We used initial conditions consistent with launch from five different points on the surface of Io; the apex, the antapex, the subjovian and antijovian points, as well as the south pole region were chosen as sources of escaping ejecta. In addition, we modeled the ejecta speed distributions using two different models, the scaling (rubble) model of Housen et al. (1983) and the spallation model of Melosh (1984, 1985, 1989) as modified by Zahnle

Author's personal copy

et al. (2008). Initial conditions for the different cases were integrated for 10,000 years using the Swift-RMVS3 (Levison and Duncan, 1994) and the fates and lifetimes of these particles were recorded. Most particles are accreted by Io itself, while between 5.0 and 8.7% reached Europa, and between 1.5 and 4.6% reached Ganymede (rubble and spall models, respectively). To transform these fractions to a mass we estimated the total amount of ejecta produced and the fraction of such ejecta that is able to escape Io. To transform this to a transfer rate we make use of Zahnle et al.'s studies of cratering rates in the outer Solar System (2003), from which we compute transfer rates of ejecta from Io to Europa and Ganymede of approximately 3.1×10^{14} and 1.6×10^{14} g on a million year time scale (the spall values—see Table 4—give us the upper limits). To put this in perspective, if the amount of mass from Io deposited on Europa over a million years were uniformly distributed over its surface, the layer would be ~3 μm thick.

There were only three test particles (all spalls) that escaped to heliocentric space; these are likely candidates to be eventually swept up by Jupiter, and only one spall and one rubble particle each that managed to survive the 10,000 year integrations (see Fig. 6).

We can summarize our work with the following simple formula for the transfer of mass from one satellite to another per unit time due to impacts as

$$\dot{m} = 4\pi R_m^2 \dot{C} f_j m_{\rm esc}, \tag{14}$$

where

- R_m is the source moon's physical radius.
- $\dot{C}$ is the cratering rate (per unit area, per unit time) in the source moon, and can be obtained from Zahnle et al. (2003).
- f_j is the fraction of the escaping ejecta from Io that reaches a given target satellite (j) and is found by numerical simulations. It is slightly different depending on the ejection model assumed (see Table 3).
- $m_{\rm esc}$ is the total amount of ejecta mass that escapes the ejecta-source moon, and is given by the analytical Eq. (11) (for Io at least, $m_{\rm esc} \approx 3m_i$).

Gladman et al. (1996) summarized the work previously done regarding the exchange of meteoroids lofted by impacts among the Solar System's terrestrial planets and the Moon. They found that their model was sufficient to explain Cosmic Ray Exposure spectra of recovered lunar and martian (SNC) meteorites, and speculated on the possibility of recovering meteorites from Mercury, Venus and Earth itself. In that work they use the term "delivery efficiency" for the factor f_j above. In this and in previous papers we have been interested in the delivery and exchange of matter in the jovian (Alvarellos et al., 2002) and saturnian (Dobrovolskis and Lissauer, 2004; Alvarellos et al., 2005) satellite systems, which can be considered miniature Solar System. We can generalize the concept of delivery efficiency by considering it to be a matrix f_{jk}, i.e., the delivery efficiency of transferring rocks from satellite j to satellite k (ignoring the smaller satellites, we set Io, Europa, Ganymede and Callisto to indices 1, 2, 3, 4, respectively). Marchi et al. (2001) provide analytical estimates of the delivery efficiencies for satellites on adjacent orbits. They then proceed to identify 'interesting' satellite-pairs in the Solar System, i.e. cases where the delivery efficiencies are >0.01, namely Titan–Hyperion (a problem studied in detail by Dobrovolskis and Lissauer, 2004) and the uranian satellites. In their work the Galilean satellites are deemed uninteresting since their simplified analysis predicts delivery efficiencies $f < 0.01$ in all adjacent pairs, unless $v_\infty > 2.4$ km/s. However, our work has shown that far from being uninteresting, a non-negligible amount of matter can be transferred between these moons in the form of impact ejecta.

Acknowledgments

We would like to acknowledge Jack J. Lissauer for useful discussions, and R.A. Jacobson for providing the initial conditions for the Jupiter system. As usual, J.L.A. would like to acknowledge the patience of Alejandra, Joselito and Isabella and Danielito. Also we would like to acknowledge Luke Dones and O.S. Barnouin-Jha for their useful and insightful reviews. This work has made use of NASA's Astrophysics Data System (ADS located at http://adswww.harvard.edu) and was written using MiKTeX ver. 2.1. We thank the NASA Exobiology Program for support.

References

Alvarellos, J.L., Zahnle, K.J., Dobrovolskis, A.R., Hamill, P., 2002. Orbital evolution of impact ejecta from Ganymede. Icarus 160, 108–123.

Alvarellos, J.L., Zahnle, K.J., Dobrovolskis, A.R., Hamill, P., 2005. Fates of satellite ejecta in the Saturn system. Icarus 178, 104–123.

Burns, J.A., Gladman, B.J., 1998. Dynamically depleted zones for Cassini's safe passage beyond Saturn's rings. Planet. Space Sci. 46, 1401–1407.

Campbell, J.K., Synnott, S.P., 1985. Gravity field of the jovian system from Pioneer and Voyager tracking data. Astron. J. 90, 364–372.

Cintala, M.J., Berthoud, L., Hörz, F., 1999. Ejection-velocity distributions from impacts into coarse-grained sand. Meteorit. Planet. Sci. 34, 605–623.

Dobrovolskis, A.R., Lissauer, J.J., 2004. The fate of ejecta from Hyperion. Icarus 169, 462–473.

Dobrovolskis, A.R., Alvarellos, J.L., Lissauer, J.J., 2007. Lifetimes of small bodies in planetocentric (or heliocentric) orbits. Icarus 188, 481–505.

Gavrilov, S.V., Zharkov, V.N., 1977. Love numbers of the giant planets. Icarus 32, 443–449.

Gladman, B.J., Burns, J.A., Duncan, M., Lee, P., Levison, H.F., 1996. The exchange of impact ejecta between the terrestrial planets. Science 271, 1387–1392.

Hamilton, D.P., Burns, J.A., 1994. Origin of Saturn's E ring: Self-sustained, naturally. Science 264, 550–553.

Horedt, G.P., Neukum, G., 1984. Planetocentric versus heliocentric impacts in the jovian and saturnian satellite systems. J. Geophys. Res. 89, 10405–10410.

Housen, K.R., Schmidt, R.M., Holsapple, K.A., 1983. Crater ejecta scaling laws: Fundamental forms based on dimensional analysis. J. Geophys. Res. 88, 2485–2499.

Jacobson, R.A., Haw, R.J., McElrath, T.P., Antreasian, P.G., 1999. A comprehensive orbit reconstruction for the Galileo prime mission in the J2000 system. AAS paper 99-330, AAS/AIAA Astrodynamics Specialist Conference, Girdwood, AK.

Johnson, T.V., Soderblom, L.A., 1982. Volcanic eruptions on Io: Implications for surface evolution and mass loss. In: Morrison, D. (Ed.), Satellites of Jupiter. Univ. of Arizona Press, Tucson, pp. 634–646.

Author's personal copy

Johnson, R.E., Carlson, R.W., Cooper, J.F., Paranicas, C., Moore, M.H., Wong, M.C., 2004. Radiation effects on the surfaces of the Galilean satellites. In: Bagenal, F., Dowling, T.E., McKinnon, W.B. (Eds.), Jupiter. Cambridge Univ. Press, Cambridge, UK, pp. 485–512.

Krivov, A.V., Krüger, H., Grün, E., Thiessenhusen, K., Hamilton, D.P., 2002. A tenuous dust ring of Jupiter formed by escaping ejecta from the Galilean satellites. J. Geophys. Res. 107, 1029–1041.

Levison, H.F., Duncan, M.J., 1994. The long-term dynamical behavior of short period comets. Icarus 108, 18–36.

Lieske, J.H., 1998. Galilean satellite ephemerides E5. Astron. Astrophys. Suppl. Ser. 129, 661–685.

Marchi, S., Dell'Oro, A., Paolicchi, P., Barbieri, C., 2001. Collisional processes and transfer of mass among the planetary satellites. Astron. Astrophys. 374, 1135–1149.

Melosh, H.J., 1984. Impact ejection, spallation and the origin of meteorites. Icarus 59, 234–260.

Melosh, H.J., 1985. Ejection of rock fragments from planetary bodies. Geology 13, 144–148.

Melosh, H.J., 1989. Impact Cratering. Oxford Univ. Press, New York.

McEwen, A.S., Preblich, B.S., Turtle, E.P., Artemieva, N.A., Golombek, M.P., Hurst, M., Kirk, R.L., Burr, D.M., Christensen, P.R., 2005. The rayed crater Zunil and interpretations of small impact craters on Mars. Icarus 176, 351–381.

Murray, C.D., Dermott, S.F., 1999. Solar System Dynamics. Cambridge Univ. Press, New York.

Schmidt, R.M., Housen, K.R., 1987. Some recent advances in the scaling of impact and explosive cratering. Int. J. Impact Eng. 5, 543–560.

Smith, B.A., and 28 colleagues, 1982. A new look at the Saturn system: The Voyager 2 images. Science 215, 504–537.

Soter, S., 1971. The dust belts of Mars. Cornell Cont. Radiophys. Space Res. Rep. 462.

Veverka, J., Thomas, P., Johnson, P.V., Matson, D., Housen, K., 1986. The physical characteristics of satellite surfaces. In: Burns, J., Mathews, M.S. (Eds.), Satellites. Univ. of Arizona Press, Tucson, pp. 342–402.

Wisdom, J., Holman, M., 1991. Symplectic maps for the n-body problem. Astron. J. 102, 1528–1538.

Zahnle, K., Dones, L., Levison, H.F., 1998. Cratering rates on the Galilean satellites. Icarus 136, 202–222.

Zahnle, K., Schenk, P., Sobieszczyk, S., Dones, L., Levison, H.F., 2001. Differential cratering of synchronously rotating satellites by ecliptic comets. Icarus 153, 111–129.

Zahnle, K., Schenk, P., Levison, H., Dones, L., 2003. Cratering rates in the outer Solar System. Icarus 163, 263–269.

Zahnle, K., Alvarellos, J.L., Dobrovolskis, A.R., Hamill, P., 2008. Secondary and sesquinary craters on Europa. Icarus 194, 660–674.

Zeehandelaar, D.B., Hamilton, D.P., 2007. A local source for the Pioneer 10 and 11 circumjovian dust detections. ESA Publications, SP-643, pp. 103–106.